iScience

CellPress
OPEN ACCESS

Article

Lemon Exosome-like Nanoparticles-Manipulated Probiotics Protect Mice from *C. diff* Infection

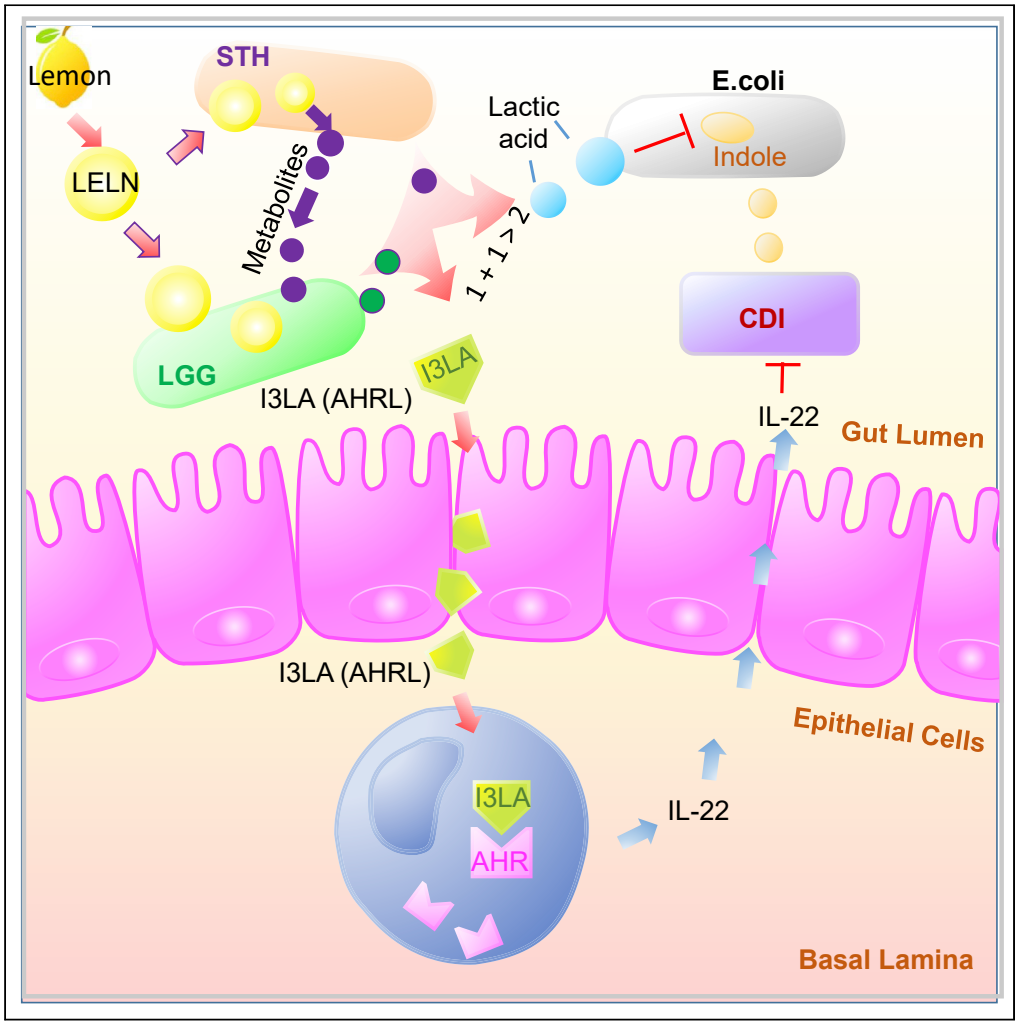

Chao Lei, Jingyao Mu, Yun Teng, ..., Craig J. McClain, Xiang Zhang, Huang-Ge Zhang

h0zhan17@louisville.edu

HIGHLIGHTS

LELNs-manipulated probiotics protect mice from *C. diff* infection

LELNs manipulation modulates gut metabolomics composition

Cross talk between LGG and STH enhances production of lactic acid and AhR ligands

Lei et al., iScience *23*, 101571 October 23, 2020
https://doi.org/10.1016/j.isci.2020.101571

iScience

CellPress
OPEN ACCESS

Article

Lemon Exosome-like Nanoparticles-Manipulated Probiotics Protect Mice from *C. diff* Infection

Chao Lei,[2] Jingyao Mu,[2] Yun Teng,[2] Liqing He,[3] Fangyi Xu,[2] Xiangcheng Zhang,[4] Kumaran Sundaram,[2] Anil Kumar,[2] Mukesh K. Sriwastva,[2] Matthew B. Lawrenz,[6,7] Lifeng Zhang,[2] Jun Yan,[2] Wenke Feng,[5] Craig J. McClain,[5] Xiang Zhang,[3] and Huang-Ge Zhang[1,2,6,8,*]

SUMMARY

Clostridioides difficile (C. diff) is the leading cause of antibiotic-associated colitis. Here, we report that lemon exosome-like nanoparticles (LELNs) manipulated probiotics to inhibit _C. diff_ infection (CDI). LELN-manipulated _Lactobacillus rhamnosus_ GG (LGG) and _Streptococcus thermophilus_ ST-21 (STH) (LELN-LS) decrease CDI mortality via an LELN-mediated increase in bile resistance and gut survivability. LELN-LS treatment increases the AhR ligands indole-3-lactic acid (I3LA) and indole-3-carboxaldehyde (I3Ald), leading to induction of IL-22, and increases lactic acid leading to a decrease of _C. diff_ fecal shedding by inhibiting _C. diff_ growth and indole biosynthesis. A synergistic effect between STH and LGG was identified. The STH metabolites inhibit gluconeogenesis of LGG and allow fructose-1,6-bisphosphate (FBP) to accumulate in LGG; accumulated FBP then activates lactate dehydrogenase of LGG (LGG-LDH) and enhances production of lactic acid and the AhR ligand. Our findings provide a new strategy for CDI prevention and treatment with a new type of prebiotics.

INTRODUCTION

Clostridioides difficile (*C. diff*) is a spore-forming opportunistic pathogen that causes diarrhea and pseudomembranous colitis in humans (Gerding et al., 1995). *C. diff* infection (CDI) is becoming a significant public health problem, especially in developed countries, associated with increasing morbidity, mortality, and medical costs (Lucado et al., 2006; Dubberke and Olsen, 2012). According to the reports of the Centers of Disease Control and Prevention, there are about 500,000 people who have CDI, which results in over 15,000 directly associated deaths per year in United States alone. Vancomycin and metronidazole are the most used antibiotics to treat CDI, with about 20%–30% recurrence after the antibiotic treatment is stopped (Stevens et al., 2017; Balsells et al., 2019). Fecal microbiota transplant (FMT) has proved to be one of most efficient methods to treat CDI and to also reduce the recurrence of CDI (Bakken et al., 2011). FMT carries increasing risks, including the risk of transmitting other infections such as HIV, hepatitis, and retrovirus; the risk of transferring superbugs with antibiotic resistance; and the risk of microbiota functional divergence in different individuals due to complex and varying composition of fecal microbiota (Wang et al., 2016). All these risks highlight the importance of developing probiotic treatments for CDI.

The concept of promoting human health through consumption of beneficial microorganisms has evolved during the last century (George Kerry et al., 2018). Numerous studies have been published under this broad definition, attempting to demonstrate beneficial effects of probiotics to CDI, however, with highly mixed results (Na and Kelly, 2011; Shen et al., 2017; Box et al., 2018). The considerable variation in outcomes between clinical trials may be attributed to multiple factors, including differences in the bacterial strains used among researchers and the survivability of the studied microorganisms in different individuals' gut microenvironment. Therefore, we urgently need to have an alternative approach to develop generalized and efficient probiotics for the prevention and treatment of CDI.

Our diet includes a variety of plants, which contain a large quantity of exosome-like nanoparticles (ELNs) of different compositions (Yang et al., 2018; Iravani and Varma, 2019). ELNs play critical roles in inter-bacterial

[1]Robley Rex Veterans Affairs Medical Center, Louisville, KY 40206, USA

[2]Department of Chemistry, University of Louisville, CTRB 309 505 Hancock Street, Louisville, KY 40202, USA

[3]Kidney Disease Program and Clinical Proteomics Center, University of Louisville, Louisville, KY, USA

[4]Department of ICU, the Affiliated Huaian NO.1 People's Hospital of Nanjing Medical University, Huaian, Jiangsu 223300, China

[5]Department of Medicine, University of Louisville, Louisville, KY 40202, USA

[6]Department of Microbiology & Immunology, University of Louisville, Louisville, KY 40202, USA

[7]Center for Predictive Medicine, University of Louisville, Louisville, KY 40202, USA

[8]Lead contact

*Correspondence: h0zhan17@louisville.edu

https://doi.org/10.1016/j.isci.2020.101571

communication (Teng et al., 2018; Sundaram et al., 2019). Therefore the manipulation of probiotics with unlimited resources of ELNs is likely to provide an opportunity to choose personalized ELNs for the optimization of probiotic therapies in general. In this study, as proof of concept, we focused on the critical issue of CDI treatments with current commercially available probiotics formulated in yogurt using *in vivo* and *in vitro* experiments. Our focus and design directly characterized the effects of the manipulation of yogurt-derived probiotics with lemon exosome-like nanoparticles (LELNs) on the protection of mice against CDI. In addition, we further explored the cellular and molecular mechanism underlying the effects.

RESULTS

LELNs Protect Mice from CDI by Enhancing the Survivability of Probiotics

Probiotic benefits are prone to be dose dependent (Bertazzoni et al., 2013), and our previous research showed that edible plant-derived nanoparticles are potent factors for increasing beneficial bacteria numbers in the gut (Teng et al., 2018). Here, using LELNs as proof of concept, we developed LELNs that manipulated probiotics in such a way to prevent and serve as a beneficial therapy for CDI. Mice were infected with *C. diff* spores as shown in Figure S1. To test the ability of the probiotics to prevent CDI, we prepared probiotic yogurt using yogurt starter #2 (YS2) and 11 strains of probiotics (11-SP). Yogurt treatment alone provided no protection to CDI in which 80% mice died in 7 days after infection, whereas LELN-yogurt treatment decreased the mortality to 40% (Figure S2A). Probiotic strains in the yogurt were grouped and treated with LELNs and the mortality evaluated for CDI mice. We confirmed that only *Streptococcus thermophilus* ST-21 (STH) and *Lactobacillus rhamnosus* LR-32 (LRH) were essential for protecting mice from CDI (Figures S2B–S2E). We also found that *Lactobacillus rhamnosus* GG (LGG), which belongs to the same species with LRH, exhibited higher inhibition efficiency to *C. diff* growth *in vitro* (Figure S2F); therefore we used LGG to replace LRH in the test probiotic mixture. LELN-pretreated probiotic mixture containing STH and LGG (LELN-LS) further decreased the mortality from 40% to 20%, whereas STH and LGG probiotic mixtures (LS) without the LELN pretreatment provided no protection to CDI (Figure 1A). We also determined colon lengths and gut barrier integrity in infected mice. The colon lengths of both control and the LS group mice were ~20% shorter than those of non-infected mice, whereas the colon lengths of LELN-LS group mice were comparable with the non-infected mice (Figure 1B). There was obvious mucus damage observed in both control and the LS group of mice, whereas the LELN-LS group mice had similar mucus morphology as non-infected mice (Figure 1C). The gut barrier integrity was also evaluated using fluorescein isothiocyanate-dextran, and a higher fluorescence signal was detected in the serum of PBS control and LS groups of mice compared with the non-infected control mice, whereas the fluorescence signal strength of LELN-LS group mice was comparable with non-infected control mice (Figure 1D).

Fruit juice increases lactobacilli survivability in gut, but the cellular and molecular mechanisms in this phenotype are still elusive. We showed that LELNs isolated from lemon extract increased bile resistance of LGG (Figure S2G). Like LGG, bile resistance of STH was also increased over 10-fold due to LELN pretreatment (Figure 1E). The data generated in *in vitro* test were further supported by the fact that LELN treatment remarkably increased the survivability of STH passing through the gastrointestinal tract as assessed by STH colony-forming unit (CFU) in the feces 24 h after gavage (Figure 1F).

LELN-LS Protects Mice from CDI in an AhR-Dependent and AhR-Independent Pathway

To further decipher the mechanism of LELN-LS protection to CDI, we performed metabolomics analysis of colon content samples of infected mice. The infected mice were sacrificed at 24 h post infection, and colon content samples were collected for metabolomics analysis. Principal-component and dendrogram analyses showed that both LS and LELN-LS treatment can significantly change colon metabolic composition; however, the changes in LELN-LS mice were more significant (Figures S3A and S3B). Pathway enrichment analysis showed that aromatic amino acid metabolism and aminoacyl-tRNA biosynthesis pathways were most affected due to LS or LELN-LS treatment (Figure S3C). To examine the metabolomics changes in detail, we conducted heatmap cluster analysis and noticed indole-3-carboxaldehyde (I3Ald) and indole-3-lactic acid (I3LA), both of which can be produced by lactobacilli strains and serve as ligands to activate AhR (Zelante et al., 2013; Cervantes-Barragan et al., 2017), were significantly increased in the LELN-LS group compared with the PBS and LS groups (Figure 2A). The concentrations of colonic I3LA and I3Ald were further confirmed by high-performance liquid chromatography (HPLC). The metabolomics analysis was in agreement with the HPLC data indicating that LELN-LS mice had much higher levels of I3Ald and I3LA than PBS controls and LS mice (Figures S3D, S3E, and 2B). Interleukin (IL)-22, a cytokine that is secreted by both $CD3^+$T cells and ILC3 in the gut and serves as a downstream gene of the AhR pathway, was proved

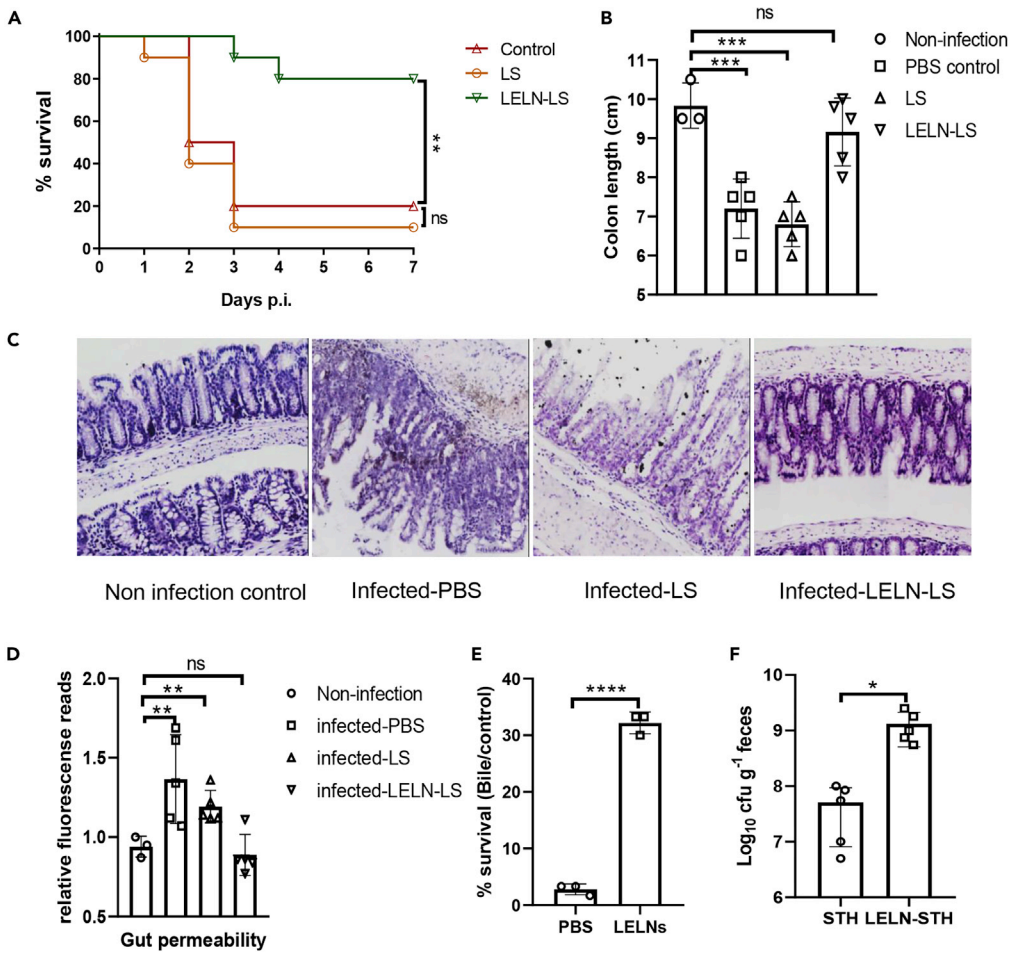

Figure 1. LELNs-Educated Probiotics Protect Mice Against *C. Diff* Infection by Increasing Probiotic Survival in the Gut

(A) Survival percentage of *C. diff*-infected mice under different treatments as indicated. PBS treatment was used as a control (n = 10).

(B) Colon lengths of *C. diff*-infected mice (n = 5).

(C) Histochemical analysis of colon tissues from *C. diff*-infected mice by H&E staining (n = 5).

(D) Gut permeability analysis measured by the fluorescein isothiocyanate -dextran method (n = 5).

(E) Survival percentage of STH under bile challenge *in vitro* with different treatments as indicated.

(F) STH and LELN-STH survivability when passing through the gastrointestinal tract.

The significance was analyzed using log rank (Mantel-Cox) tests for survival analyses, t tests for two-group analyses, and ANOVA for multiple group analyses. The significance is shown as *p ≤ 0.05, **p ≤ 0.01, ***p ≤ 0.001, and ****p ≤ 0.0001. p > 0.05 was considered to be not significant (ns). Data are shown as mean ± SD. See also Figure S2.

to be important in the protection of the host from infection (Parks et al., 2015). Our confocal imaging data also suggest that IL-22 is detected in $CD3^{+}$T cells and ILC3 cells (Figures S4A and S4B). qPCR analysis indicates that IL-22 mRNA levels in colon tissue were found to be upregulated over 4-fold in LELN-LS mice and only by 1.5-fold in the LS mice compared with the PBS control mice (Figure 2C). Neither LS nor LELN-LS treatments changed the AhR expression in the colon (Figure 2C). IL-22 protein levels in the small intestine and colon mucus were determined by ELISA. The IL-22 protein levels in the small intestine were shown to be increased from 24 ± 8.5 to 56 ± 6.5 pg/mL and 107 ± 27.6 pg/mL in LS mice and LELN-LS mice, respectively. The colonic IL-22 protein levels were increased from 57 ± 46 to 134 ± 17 pg/mL in LELN-LS mice, but colonic IL-22 protein levels of LS mice were comparable with those of the PBS mice (Figure 2D). To verify the protection effect of I3Ald and I3LA in CDI, I3Ald or I3LA were given to mice via their drinking water at a concentration of 1 mM. Both I3LA and I3Ald increased the survival percentage from 20% to 40% in wild-type C57BL/6 mice (Figure 2E), whereas all the AhR knockout mice ($AhR^{-/-}$), including I3LA- and I3Ald-treated

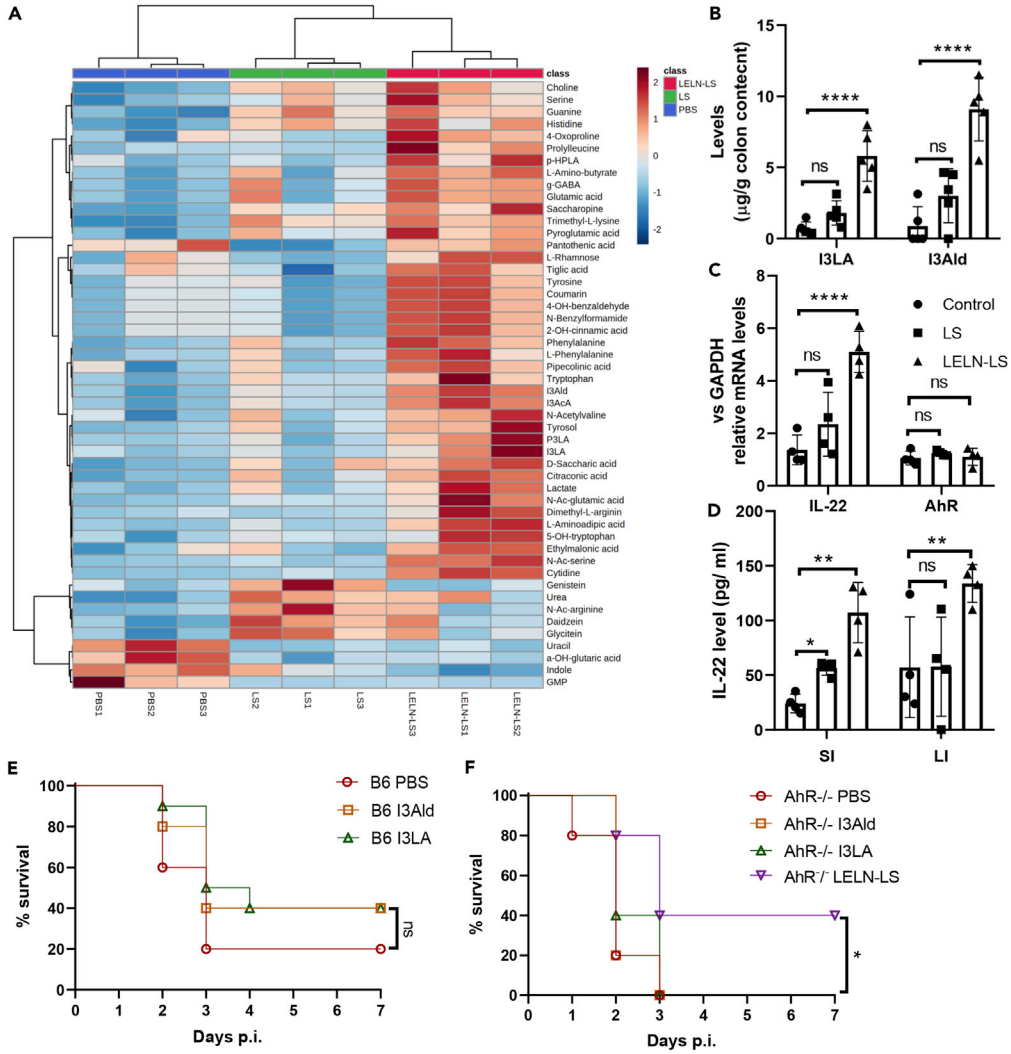

Figure 2. LELN-LS Protects Mice from *C. diff* Infection Partially via the AhR Pathway

(A) Colon contents metabolomics analysis of *C. diff*-infected mice with different treatments as indicated. The metabolomics data were normalized by autoscaling (mean-centered and divided by standard deviation), and further transformed with log2. The top 50 most changed metabolites were listed in the heatmap.

(B) Confirmation of the concentration of I3Ald and I3LA in the colon content samples using HPLC analysis.

(C) Relative mRNA levels of IL-22 and AhR in the colon tissue determined by real-time qPCR; GAPDH were used as internal reference.

(D) IL-22 protein levels in the mucus of the small intestine (SI) and colon (LI) determined by ELISA.

(E and F) Percent survival of *C. diff*-infected mice with I3Ald, I3LA, or LELN-LS treatment; both wild-type (E) and AhR knockout (F) C57BL/6 mice were tested.

The significance was analyzed using log rank (Mantel-Cox) tests for survival analyses, t tests for two-group analyses, and ANOVA for multiple group analyses. The significance is shown as *$p \leq 0.05$, **$p \leq 0.01$, and ****$p \leq 0.0001$. $p > 0.05$ was considered to be not significant (ns). Data are shown as mean ± SD. See also Figure S3.

mice died 3 days after being infected (Figure 2F). As both interferon (IFN)-γ and IL-17 were reported to be important to protect against CDI (Chen et al., 2020; Abt et al., 2015), we thus tested whether LELN-LS administration increases IFN-γ and IL-17 expressed in the gut. No significant difference was found in both IFN-γ and IL-17 levels among the groups tested (Figures S4C–S4F). To confirm whether LELN-LS protected mice from CDI only by the AhR pathway, we pretreated AhR$^{-/-}$ mice with LELN-LS and conducted a *C. diff* infection study. All the mice in the PBS control group died within 3 days of being infected, whereas 40% of the LELN-LS group were alive 7 days after being infected (Figure 2F), indicating that an AhR-independent pathway contributes to LELN-LS-mediated protection of mice to CDI.

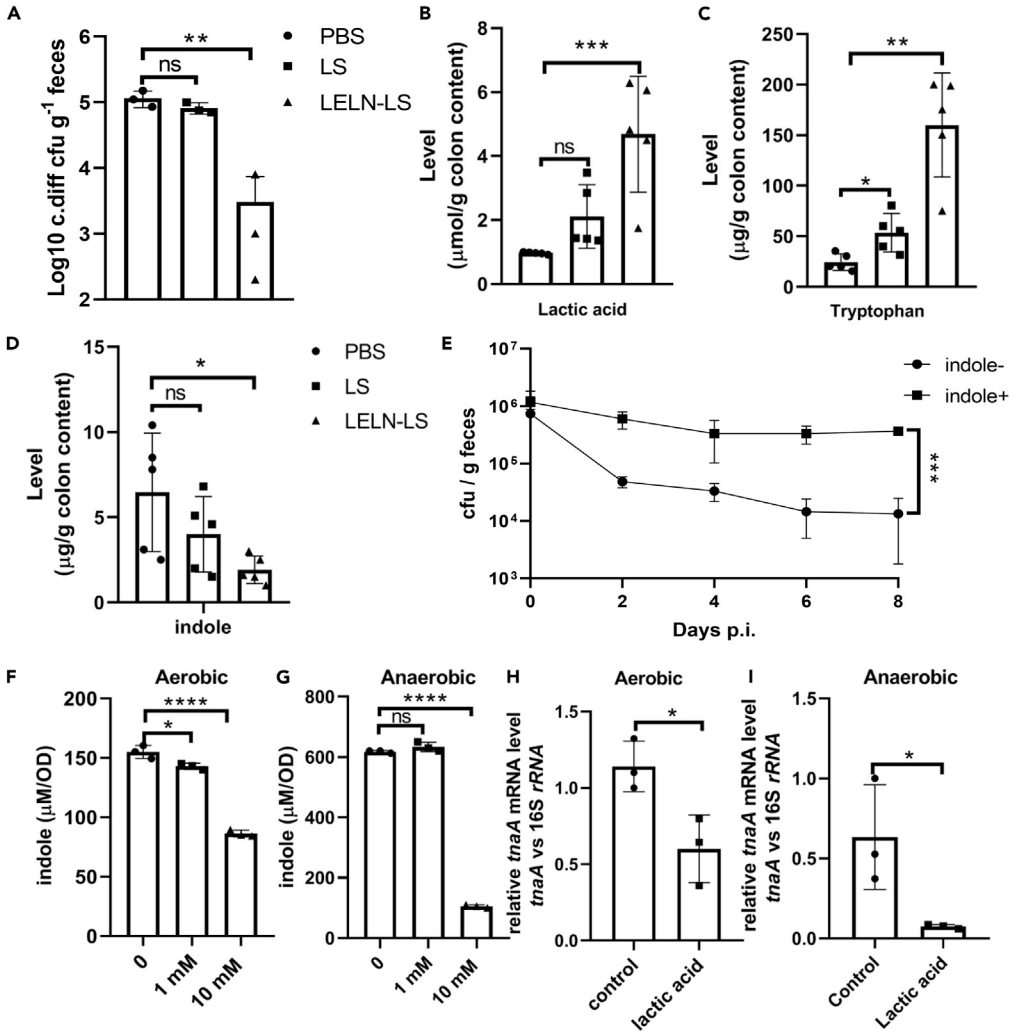

Figure 3. LELN-LS Decreases *C. diff* Shedding in Mouse Feces by Altering the Composition of the Intestinal Metabolites

(A) Enumeration of *C. diff* CFUs in the feces of *C. diff*-infected mice with different treatments.

(B) Lactic acid concentration in the colon contents of *C. diff*-infected mice.

(C and D) (C) Tryptophan and (D) indole concentrations in the colon contents of *C. diff*-infected mice.

(E) *C. diff* CFUs in the feces of *C. diff*-infected mice with or without 1 mM indole in drinking water.

(F and G) Lactic acid effects on indole production in *E. coli* under (F) aerobic and (G) anaerobic culture conditions; two different concentrations of lactic acid were added to the *E. coli* cultures as indicated.

(H and I) Lactic acid effect on expression of the indole biosynthesis gene *tnaA* under (H) aerobic and (I) anaerobic culture conditions, 10 mM of lactic acid were used in the tests. 16s rRNA gene were used as internal reference for relative quantification.

The significance was analyzed using t tests for two-group analyses and ANOVA for multiple group analyses. The significance is shown as *$p \leq 0.05$, **$p \leq 0.01$, ***$p \leq 0.001$, and ****$p \leq 0.0001$. $p > 0.05$ was considered to be not significant (ns). Data are shown as mean ± SD. See also Figure S5.

LELN-LS Decreases *C. diff* Shedding by Altering the Composition of Intestinal Metabolites

C. diff shedding in feces is a primary factor in the transmission of CDI and a major issue in preventing the spread. *C. diff* shedding in the feces of infected mice was determined as a means to study the LELN-LS protection mechanism. Feces were collected from surviving mice on day 7 after infection and CFUs of *C. diff* were determined by plating on TCCF agar. LS treatment slightly decreased *C. diff* CFUs compared with the PBS control group, whereas LELN-LS treatment decreased *C. diff* CFUs by nearly two orders of magnitude (Figure 3A). We then tested whether metabolites from LS directly inhibit *C. diff* growth *in vitro*. LS culture

supernatant inhibited *C. diff* growth in a dose-dependent manner (Figure S5A). We also tested whether metabolites from cecum inhibited *C. diff* growth *in vitro*. Supernatant from cecum contents were added into the *C. diff* inoculum (10% by volume). Only the supernatant from the LELN-LS mice cecum content exhibited significant inhibitory effect on *C. diff* growth (Figure S5B). Both LGG and STH produce lactic acid as an end fermentation product, and lactic acid has been reported to inhibit a large variety of pathogens (Vieco-Saiz et al., 2019). We tested whether lactic acid inhibits *C. diff* growth *in vitro*. Lactic acid was found to inhibit *C. diff* growth efficiently with a minimum inhibitory concentration of 40 mM (Figure S5C). Metabolomics analysis of colon content samples showed lactate levels being significantly increased in the LELN-LS-treated mice (Figure 2A). The lactate concentration in colon content samples was further confirmed using a lactate detection kit. The lactate level in colon content of LELN-LS mice was increased ~ 4-fold compared with the PBS control mice, whereas there was only a slight but not significant increase in the LS mice (Figure 3B).

We also noticed decreasing levels of indole along with increasing levels of tryptophan in the colon based on metabolomics analysis and confirmed by HPLC (Figures 2A, S3E, 3C, and 3D). Recent research indicates that indole levels are increased in patients with CDI, and the authors inferred that indole might play a role in *C. diff* survival by modulating the gut microbiota (Vieco-Saiz et al., 2019). We propose that LELN-LS can decrease the *C. diff* burden by inhibiting production of indole in the gut. To test this hypothesis, we challenged mice with a lower dose of 10 *C. diff* spores to avoid a high mortality. After recovering from an initial diarrhea (day 4 after infection), mice were treated with LELN-LS with or without indole in their drinking water. *C. diff* numbers in the feces were counted every 2 days for a total of 8 days. *C. diff* numbers in the LELN-LS control mice decreased significantly over time, whereas *C. diff* numbers in the indole-treated group persisted at a high level throughout the analysis period (Figure 3E). To further understand the mechanism as to how LELN-LS downregulates indole levels in the gut, we tested the effect of lactic acid on indole biosynthesis in *E. coli*, which is one of the primary indole producers in the gut (Kumar and Sperandio, 2019). We first tested lactic acid effect on *E. coli* growth by measuring growth curve. We found that lactic acid only slightly inhibited *E. coli* growth at a concentration of 10 mM, whereas 1 mM of lactic acid had no effect on *E. coli* growth (Figure S5D). We then tested lactic acid effect on indole biosynthesis. We found that a lactic acid concentration of 10 mM can decrease indole levels in *E. coli* culture broth in both aerobic and anaerobic conditions and lactic acid showed stronger inhibition of indole biosynthesis in anaerobic growth conditions (Figures 3F and 3G). We further tested the effect of lactic acid on the expression of the indole biosynthesis gene *tnaA*. Lactic acid with indicated concentrations were added into *E. coli* culture when OD600 reaches 0.6, bacteria were collected to isolate total RNA at 2 h after addition of lactic acid. Lactic acid at a concentration of 10 mM decreased *tnaA* expression ~ 2-fold in aerobic conditions and over 4-fold in anaerobic conditions (Figures 3H and 3I). To confirm if lactic acid regulation to *tnaA* expression is specific, we also tested another housekeeping gene *rpoD*, which is not affected by lactic acid. Collectively, these data suggest that LELN-LS treatment leads to increasing the amount of intestinal lactic acid, which subsequently causes a decrease in the production of indole, which is a survival factor for *C. diff*. This occurs due to inhibition of the expression of the indole biosynthesis gene *tnaA*.

Co-LS Increases FBP-Mediated LDH Activity and Promotes Production of Lactic Acid and I3LA

It is interesting that neither LELNs-pretreated STH nor LELNs-pretreated LGG alone was sufficient to protect mice from CDI (Figure S6A); this indicates a synergetic effect between these two strains. We found that supernatant from *in vitro* co-cultures of STH and LGG without LELNs (Co-LS) exhibited higher inhibition efficiency to *C. diff in vitro* compared with pure culture (Figure S6B). We then quantified lactic acid in the broth from LGG, STH, and Co-LS and found Co-LS broth contained higher concentrations of lactic acid than when STH and LGG were cultured separately (Figure 4A). Metabolomics analysis of supernatant from LGG, STH, and Co-LS cultures was performed to analyze the metabolic changes under co-culture conditions. We found that a number of organic acids including lactic acid (LA), p-hydroxyphenyllactic acid (p-HPLA), phenyl-3-lactic acid (P3LA), and I3LA were increased significantly in Co-LS supernatant (Figure 4B). We confirmed the concentration of I3LA in the broth by HPLC, which is consistent with the metabolomics analysis result (Figure 4C). p-HPLA, P3LA, and I3LA have a common biosynthesis pathway in the aryl-lactic acid group, and LA can be biosynthesized by lactate dehydrogenase (LDH) from pyruvic acid (Figure S7). Based on this information we tested whether LDH can convert aryl-pyruvic acid into aryl-lactic acid using an *in vitro* assay. Using commercially available LDH derived from *Lactobacillus leichmannii*, we successfully transformed I3PA to I3LA, with NADH as a cofactor (Figure 4D). We also noticed that I3PA is very unstable, especially at a lower pH such as pH4.5, and prone to degrade into I3Ald when LDH is absent (Figure S8A).

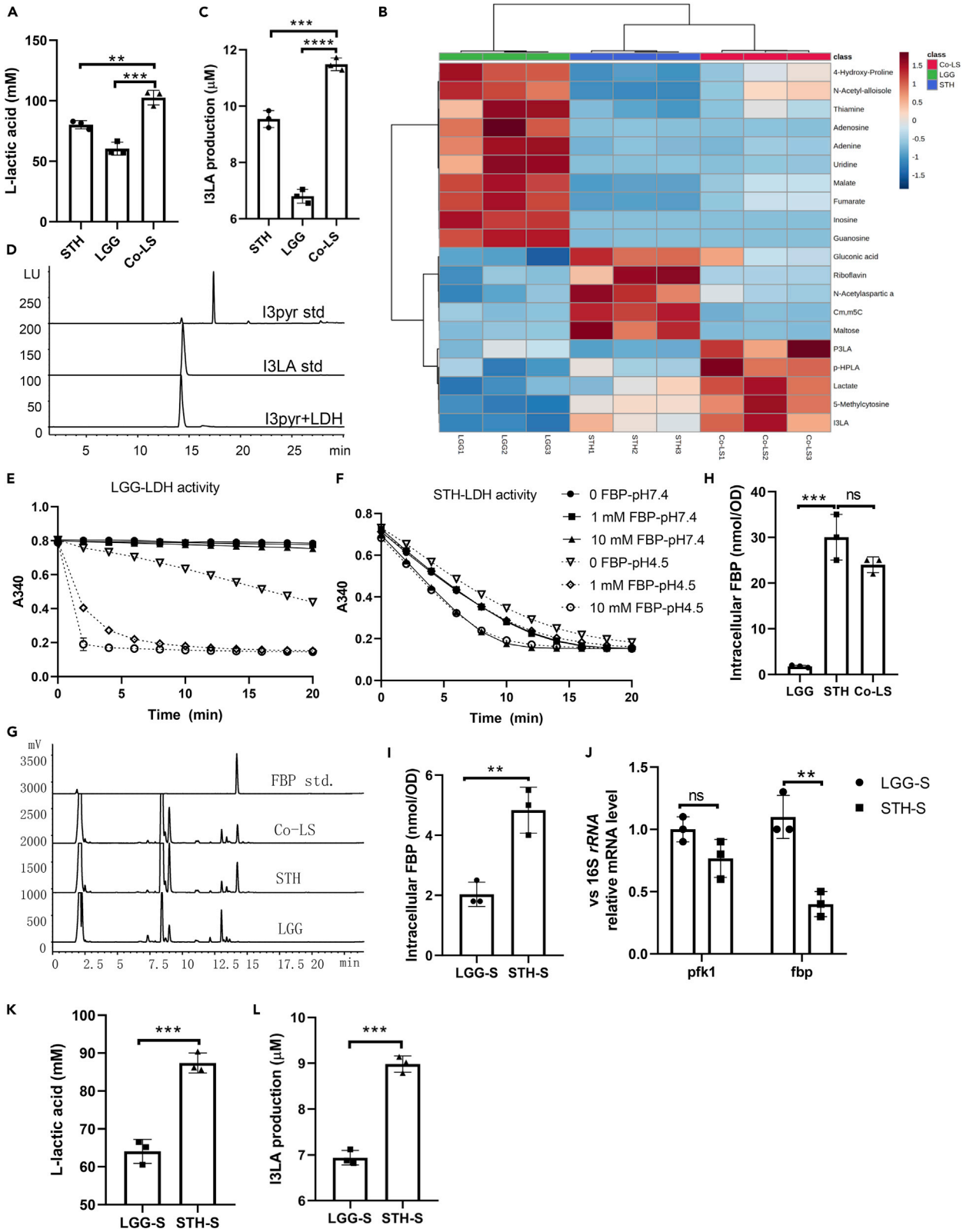
A
L-lactic acid (mM)
STH
LGG
Co-LS
C
I3LA production (μM)
B
class
Co-LS
LGG
STH
4-Hydroxy-Proline
N-Acetyl-alloisole
Thiamine
Adenosine
Adenine
Uridine
Malate
Fumarate
Inosine
Guanosine
Gluconic acid
Riboflavin
N-Acetylaspartic a
Cm,m5C
Maltose
P3LA
p-HPLA
Lactate
5-Methylcytosine
I3LA
D
LU
I3pyr std
I3LA std
I3pyr+LDH
min
E
LGG-LDH activity
A340
Time (min)
F
STH-LDH activity
0 FBP-pH7.4
1 mM FBP-pH7.4
10 mM FBP-pH7.4
0 FBP-pH4.5
1 mM FBP-pH4.5
10 mM FBP-pH4.5
H
Intracellular FBP (nmol/OD)
ns
G
mV
FBP std.
Co-LS
STH
LGG
I
J
vs 16S rRNA relative mRNA level
LGG-S
STH-S
pfk1
fbp
K
L

Figure 4. STH Metabolites Activate LGG-LDH and Produce More Lactic Acid and I3LA when in Co-culture

(A) Lactic acid concentration in the supernatants of bacterial cultures without LELNs.

(B and C) (B) Metabolomics analysis of supernatants from different bacteria cultured as indicated. The metabolomics data were normalized by autoscaling and further transformed with log2. The top 20 most changed metabolites among groups are listed. (C) Confirmation by HPLC of I3LA concentration in culture supernatants.

(D) *In vitro* transformation of I3PA to I3LA by the catalysis of LDH.

(E and F) Total LDH activities of (E) LGG and (F) STH under different pH and different concentrations of FBP as indicated.

(G) HPLC analyses of intracellular FBP concentration. (H) Statistic analysis of intracellular FBP concentration determined by HPLC.

(I) Intracellular FBP concentration of LGG shocked with the supernatant from LGG or STH overnight cultures.

(J) Relative mRNA levels of pfk1 and fbp in LGG with indicated treatments, 16S-rRNA was used as internal reference gene for real-time PCR analysis.

(K and L) (K) Lactic acid and (L) I3LA production of LGG treated with supernatant from LGG or STH. All *in vitro* cultures were conducted without LELN.

The significance was analyzed using t tests for two-group analyses and ANOVA for multiple group analyses. The significance is shown as $^{**}p \leq 0.01$, $^{***}p \leq 0.001$, and $^{****}p \leq 0.0001$. $p > 0.05$ was considered to be not significant (ns). Data are shown as mean ± SD. See also Figures S6 and S8.

We thus propose an I3Ald and I3LA biosynthesis pathway in LGG and STH, involving aromatic amino acid aminotransferase (ArAT), LDH, and spontaneous degradation (Figure S8B).

We then tested whether Co-LS increases the total LDH activity using an *in vitro* assay. Total LDH activities from bacteria lysates were tested in two different buffer systems, 1X PBS buffer @ pH7.4 and 50 mM acetate buffer @ pH4.5. We found Co-LS exhibited the highest total LDH activity in both buffers tested (Figures S9A and S9B). We also found that the LDH activity of LGG (LGG-LDH) is pH dependent, whereas STH-LDH is pH independent (Figures S9A–S9C). FBP was reported to be an LDH allosteric activator (Garvie, 1980); we thus tested whether FBP activates LGG-LDH and STH-LDH in an *in vitro* assay. We found that LGG-LDH is remarkably activated by FBP at both concentrations we tested, 1 mM and 10 mM at a pH4.5, whereas STH-LDH was just slightly activated by FBP (Figures 4E and 4F). We then determined the intracellular FBP concentration of LGG, STH, and Co-LS by HPLC and found that the concentration of intracellular FBP in STH is much higher than LGG, whereas intracellular FBP concentration in Co-LS is comparable with STH (Figures 4G and 4H). To test whether metabolites from STH benefit FBP accumulation in LGG, we shocked a stationary-phase LGG culture with STH culture supernatant and noticed that the intracellular concentration of FBP in LGG was increased when compared with being shocked with LGG culture supernatant (Figure 1I). We then tested the expression of two FBP metabolism enzymes, phosphofructokinase-1 (*pfk1, LGG_01374*) and fructose bisphosphatase (*fbp,* LGG_02032), to understand the mechanism of STH metabolites benefit. We found the *fbp,* which converts FBP to fructose-6-phosphate (F6P), is the main rate-limiting enzyme in the gluconeogenesis pathway (Ganapathy et al., 2015), and it was decreased significantly due to STH supernatant shock (Figure 1J), which explains the increase of intracellular FBP of LGG. Finally, we tested whether supernatant from STH increases lactic acid and I3LA productions in LGG. Indeed, we found that STH supernatant treatment increased both lactic acid and I3LA production ~30% in LGG (Figures 4K and 4L).

DISCUSSION

In this study we demonstrate that LELNs-manipulated probiotics can inhibit CDI through both AhR-dependent and AhR-independent pathways (Figure 5). We found that maintaining sufficient numbers of probiotics in the intestine is essential for protecting against CDI, and LELNs serve as a potential prebiotic to remarkably increase probiotic survivability in the gut, thus protecting mice from CDI and fecal shedding. Our study opens a new approach to manipulate well-characterized probiotics, such as LGG and STH, with an unlimited resource of edible plant ELNs in a personalized fashion because the gut microenvironment is different in individuals.

Various types of harsh gut environmental conditions, particularly in the stomach and small intestine, could be detrimental for the survival of many types of probiotics (Dodoo et al., 2017). In the small intestine, bile acids affect probiotic viability (Wahlstrom et al., 2016). The main functions of bile acids in the lumen are exhibiting antibacterial properties, acting as detergents that disrupt cell membranes, as well as functioning as DNA-damaging agents (Merritt and Donaldson, 2009). Our finding that uptaking LELN leads to increasing survivability of LGG and STH could be due to inducing tolerance to a number of harsh gut environmental conditions inducing bile resistance. Therefore, our finding will provide a foundation for further determining whether LELN-LS also develops resistance to other harsh gut environmental conditions and identifying the molecular mechanism underlying how anti-bile acid of these probiotics is induced by LELNs.

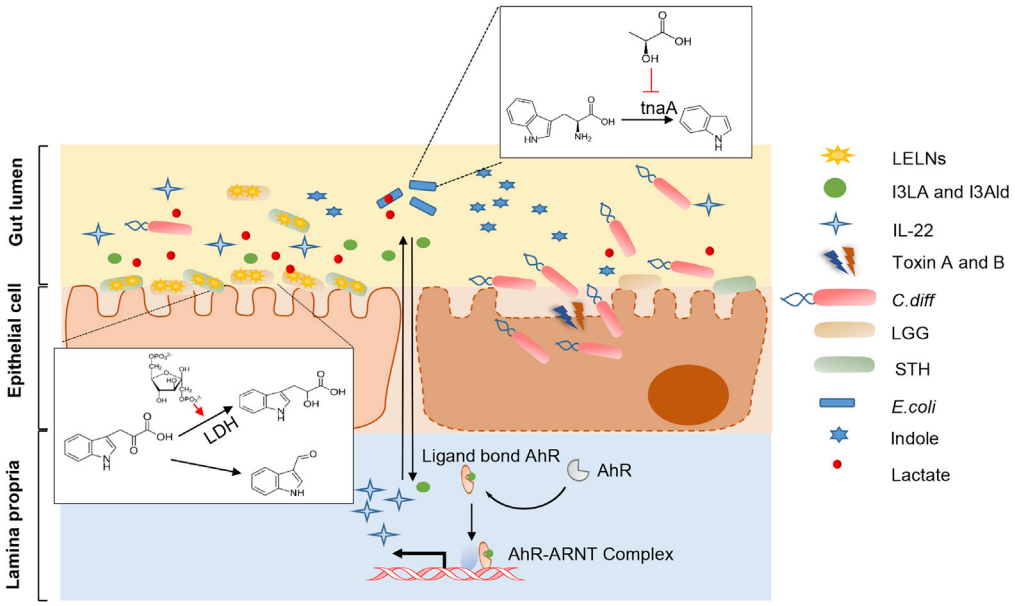

Figure 5. Diagram of LELNs-Educated Probiotics to Protect Mice Against *C. diff* Infection

LELNs manipulation increase both LGG and STH survival rate in the gut, which lead to increase production of AhR ligands I3Ald and I3LA, and lactic acid. I3Ald and I3LA induce more IL-22 to protect mice from CDI by activating AhR pathway. On the other hand, lactic acid protected from CDI by directly inhibiting *C.diff* growth and inhibiting indole biosynthesis. Metabolites from STH can inhibit LGG gluconeogenesis pathway to increase production of I3LA and lactic acid when co-culturing these two strains, thus exhibiting a synergistic effect in protecting against CDI.

Our study shows that LELN-LS treatment increases I3Ald and I3LA levels, whereas decreases the levels of indole in the gut. I3Ald and I3LA act as AhR ligands and activate AhR, which in turn activates IL-22 expression. IL-22 plays critical roles in reducing the severity of many gut infections (Valeri and Raffatellu, 2016). Our research has shown that IL-22 knockout mice exhibit much more severe symptoms upon CDI (data not shown). Meanwhile, LELN-LS treatment also leads to a decrease in indole levels (also an AhR ligand) in the colon; indole is not a high-affinity ligand for AhR in mice (Hubbard et al., 2015). These results provide a foundation for further studying whether genes induced by I3Ald and I3LA are different from the gene(s) induced by indole, which results in the different biological effects on the AhR+ recipient cells. In addition, indole is predominately detected in the large intestine, whereas I3Ald and I3LA are detected in the small and large intestine according to lactobacilli distribution in the gut. This helps explain our data where the fold increase of IL-22 in the colon is lower than the fold increase in the small intestine as a result of LELN-LS treatment.

Besides the AhR-mediated pathway that protects mice from CDI, other pathways have been recognized as well for protection of mice from CDI, including innate and adaptive immune responses (Hughes et al., 2016; Solomon, 2013). Our results showed that indole is a survival factor for *C. diff* and production of bacterial indole is inhibited by lactic acid induced by LELN-LS treatment. In addition, indole is a quorum-sensing molecule (Kumar and Sperandio, 2019; Lee and Lee, 2010) and may have critical impact on gut microbiota composition, resulting in a favorable growth environment for *C.diff*, whereas LELN-LS treatment changes gut microenvironment to handicap *C.diff* growth.

Although we demonstrated that LELNs renders bile resistance of the probiotics, other properties of LELNs recipient could be also altered, collectively contributing to anti-CDI as we demonstrated in this study. Probiotics are live organisms that confer health benefits on the host when accumulated in the right location in the intestine in adequate amounts, by bringing the microbial balance in the system, and modulating host immune response to inhibit the growth of pathogenic organisms such as *C. diff* through different mechanisms such as adherence to epithelial cells, modulation of the immune system, and secretion of antimicrobial compounds (Kechagia et al., 2013). Unlike other single factors through which it is almost impossible to alter multiple properties of probiotics, simultaneously, edible plant ELNs consist of proteins, lipids, and nuclear acids, in particular microRNAs, (Sundaram et al., 2019; Teng et al., 2018) and are capable of altering a

number of biological activities by targeting multiple factors in ELN recipient probiotics, simultaneously. Hence, our approach will provide a strategy for enhancing the survivability of probiotics like other technology such as encapsulating the probiotics in a colon-targeting polymer, and ELN itself contributes to the beneficial effect on the host by possibly targeting multiple pathways of the probiotics. In addition, unlike polymer, because ELN is derived from the diet we take, there will be much less consideration of the side effects. Therefore, our results presented in this study also open a new avenue to investigate the effect of ELN, in general, on the improvement of probiotic's beneficial properties besides inducing bile acid resistance.

It is well recognized that gut microbiota-derived metabolites have huge impact on our overall health (Owyang and Wu, 2014). Our results showed that LELN treatment leads to altering the composition of LELN recipient metabolites; it is conceivable that these altered metabolites may contribute to anti-CDI by modulating not only the activity of gut microbiota near LELN-recipient probiotics but also host cellular activity when they are increased systemically.

However, we must be careful about drawing any final conclusions regarding *in vivo* application based on data generated from an *in vitro* study. As we demonstrated in this study, *in vitro* data show that co-culture of LGG and STH leads to the highest level of lactic acid, which inhibits *C. diff* growth. However, oral administration of LGG and STH (LS) without LELN treatment does not prevent CDI (Figure 1A). This discrepancy is likely due to the probability that the number of LGG and STH probiotic gavage given decreases dramatically while traversing through the intestine (Figure 1F), which limits the amount of beneficial factors that are generated, including lactic acid (Figures 2A and 3B). LELNs pretreatment is necessary to enhance the survivability of STH and LGG so that an ample level of lactic acid is produced to prevent *C. diff* growth *in vivo* and inhibit indole biosynthesis.

Combinations of different probiotics for acquiring better health benefits have been attempted, although little is known about the mechanism of benefit. Our study indicates a synergistic effect between LGG and STH, both of which are essential to protect against CDI. STH is an important industrial strain that is widely used in yogurt and cheese production to accomplish fast acidification (Dandoy et al., 2011). Contrary to LGG-LDH whose activity is pH dependent, our data showed that STH-LDH is pH independent, which is important for allowing the accumulation of lactic acid and fast acidification. LDH may be another factor other than PrtS (Dandoy et al., 2011) that contributes to fast acidification. In addition, we found that the metabolites of STH can inhibit the expression of *fbp*, the key enzyme in the gluconeogenesis pathway (Ganapathy et al., 2015), and that the reduction of *fbp* in LGG results in the accumulation of FBP, subsequently activating LGG-LDH. Therefore, our research provides insights not only into the combined usage of probiotics but also into new ideas for future research on the interaction of combined probiotics via a metabolomics approach.

Limitations of the Study

Although our research showed that LELN increases bile resistance of probiotics LGG and STH, further research needs to be done to dissect out the molecular mechanisms underlying the LELN-mediated cross talk between LGG and STH.

Resource Availability

Lead Contact

Further information and requests for resources and reagents should be directed to and will be fulfilled by the Lead Contact, Prof. Huang-Ge Zhang (h0zhan17@louisville.edu).

Materials Availability

This study did not generate new unique reagents.

Data and Code Availability

This study did not generate datasets/code.

METHODS

All methods can be found in the accompanying Transparent Methods supplemental file.

SUPPLEMENTAL INFORMATION

Supplemental Information can be found online at https://doi.org/10.1016/j.isci.2020.101571.

ACKNOWLEDGMENTS

Dr. J. Ainsworth for editorial assistance. Funding: This work was supported by a grant from the National Institutes of Health (NIH) (R01AT008617). H.-G.Z. is supported by a Research Career Scientist (RCS) Award and NIH grants (P20GM125504, Richard J. Lamont [P.I.], P20GM13500, Craig J. McClain [P.I.]).

AUTHOR CONTRIBUTIONS

C.L. and H.-G.Z. designed the study, analyzed and interpreted the data and prepared the manuscript; C.L. performed the experiments and interpreted the data; L.H and Xiang Zhang performed metabolomics analysis; J.M., F.X., and Xiangcheng Zhang provided histological analysis; A.K., K.S., L.Z., W.F., M.L., C.M., and J.Y interpreted the findings.

DECLARATION OF INTERESTS

The authors declare no competing interests.

Received: June 30, 2020
Revised: August 13, 2020
Accepted: September 13, 2020
Published: October 23, 2020

REFERENCES

Abt, M.C., Lewis, B.B., Caballero, S., Xiong, H., Carter, R.A., Susac, B., Ling, L., Leiner, I., and Pamer, E.G. (2015). Innate immune defenses mediated by two ILC subsets are critical for protection against acute clostridium difficile infection. Cell Host Microbe *18*, 27–37.

Bakken, J.S., Borody, T., Brandt, L.J., Brill, J.V., Demarco, D.C., Franzos, M.A., Kelly, C., Khoruts, A., Louie, T., Martinelli, L.P., et al. (2011). Treating Clostridium difficile infection with fecal microbiota transplantation. Clin. Gastroenterol. Hepatol. *9*, 1044–1049.

Balsells, E., Shi, T., Leese, C., Lyell, I., Burrows, J., Wiuff, C., Campbell, H., Kyaw, M.H., and Nair, H. (2019). Global burden of Clostridium difficile infections: a systematic review and meta-analysis. J. Glob. Health *9*, 010407.

Bertazzoni, E., Donelli, G., Midtvedt, T., Nicoli, J., and Sanz, Y. (2013). Probiotics and clinical effects: is the number what counts? J. Chemother. *25*, 193–212.

Box, M.J., Ortwine, K.N., Goicoechea, M., and Stewardship, S.A. (2018). No impact of probiotics to reduce clostridium difficile infection in hospitalized patients: a real-world experience. Open Forum Infect. Dis. *5*, ofy192.

Cervantes-Barragan, L., Chai, J.N., Tianero, M.D., Di Luccia, B., Ahern, P.P., Merriman, J., Cortez, V.S., Caparon, M.G., Donia, M.S., Gilfillan, S., et al. (2017). Lactobacillus reuteri induces gut intraepithelial CD4(+)CD8alphaalpha(+) T cells. Science *357*, 806–810.

Chen, Y.S., Chen, I.B., Pham, G., Shao, T.Y., Bangar, H., Way, S.S., and Haslam, D.B. (2020). IL-17-producing gammadelta T cells protect against clostridium difficile infection. J. Clin. Invest. *130*, 2377–2390.

Dandoy, D., Fremaux, C., De Frahan, M.H., Horvath, P., Boyaval, P., Hols, P., and Fontaine, L. (2011). The fast milk acidifying phenotype of Streptococcus thermophilus can be acquired by natural transformation of the genomic island encoding the cell-envelope proteinase PrtS. Microb. Cell Fact. *10*, S21.

Dodoo, C.C., Wang, J., Basit, A.W., Stapleton, P., and Gaisford, S. (2017). Targeted delivery of probiotics to enhance gastrointestinal stability and intestinal colonisation. Int. J. Pharm. *530*, 224–229.

Dubberke, E.R., and Olsen, M.A. (2012). Burden of clostridium difficile on the healthcare System. Clin. Infect. Dis. *55*, S88–S92.

Ganapathy, U., Marrero, J., Calhoun, S., Eoh, H., De Carvalho, L.P.S., Rhee, K., and Ehrt, S. (2015). Two enzymes with redundant fructose bisphosphatase activity sustain gluconeogenesis and virulence in Mycobacterium tuberculosis. Nat. Commun. *6*, 7912.

Garvie, E.I. (1980). Bacterial lactate dehydrogenases. Microbiol. Rev. *44*, 106–139.

George Kerry, R., Patra, J.K., Gouda, S., Park, Y., Shin, H.S., and Das, G. (2018). Benefaction of probiotics for human health: a review. J. Food Drug Anal. *26*, 927–939.

Gerding, D.N., Johnson, S., Peterson, L.R., Mulligan, M.E., and Silva, J. (1995). Clostridium-difficile-associated diarrhea and colitis. Infect. Control Hosp. Epidemiol. *16*, 459–477.

Hubbard, T.D., Murray, I.A., Bisson, W.H., Lahoti, T.S., Gowda, K., Amin, S.G., Patterson, A.D., and Perdew, G.H. (2015). Adaptation of the human aryl hydrocarbon receptor to sense microbiota-derived indoles. Sci. Rep. *5*, 12689.

Hughes, M., Qazi, T., Berg, A., Weinberg, J., Chen, X., Kelly, C.P., and Farraye, F.A. (2016). Host immune response to clostridium difficile infection in inflammatory bowel disease patients. Inflamm. Bowel Dis. *22*, 853–861.

Iravani, S., and Varma, R.S. (2019). Plant-derived edible nanoparticles and miRNAs: emerging frontier for therapeutics and targeted drug-delivery. Acs Sustain. Chem. Eng. *7*, 8055–8069.

Kechagia, M., Basoulis, D., Konstantopoulou, S., Dimitriadi, D., Gyftopoulou, K., Skarmoutsou, N., and Fakiri, E.M. (2013). Health benefits of probiotics: a review. ISRN Nutr. *2013*, 481651.

Kumar, A., and Sperandio, V. (2019). Indole signaling at the host-microbiota-pathogen interface. mBio *10*, e01031-19.

Lee, J.H., and Lee, J. (2010). Indole as an intercellular signal in microbial communities. FEMS Microbiol. Rev. *34*, 426–444.

Lucado, J., Gould, C., and Elixhauser, A. (2006). Clostridium Difficile Infections (CDI) in Hospital Stays, 2009: Statistical Brief #124. Healthcare Cost and Utilization Project (HCUP) Statistical Briefs (Agency for Healthcare Research and Quality).

Merritt, M.E., and Donaldson, J.R. (2009). Effect of bile salts on the DNA and membrane integrity of enteric bacteria. J. Med. Microbiol. *58*, 1533–1541.

Na, X., and Kelly, C. (2011). Probiotics in Clostridium difficile infection. J. Clin. Gastroenterol. *45*, S154–S158.

Owyang, C., and Wu, G.D. (2014). The gut microbiome in health and disease. Gastroenterology *146*, 1433–1436.

Parks, O.B., Pociask, D.A., Hodzic, Z., Kolls, J.K., and Good, M. (2015). Interleukin-22 signaling in the regulation of intestinal health and disease. Front. Cell Dev. Biol. *3*, 85.

Shen, N.T., Maw, A., Tmanova, L.L., Pino, A., Ancy, K., Crawford, C.V., Simon, M.S., and Evans, A.T. (2017). Timely use of probiotics in hospitalized adults prevents clostridium difficile infection: a systematic review with meta-regression analysis. Gastroenterology *152*, 1889–1900.e9.

Solomon, K. (2013). The host immune response to Clostridium difficile infection. Ther. Adv. Infect. Dis. *1*, 19–35.

Stevens, V.W., Nelson, R.E., Schwab-Daugherty, E.M., Khader, K., Jones, M.M., Brown, K.A., Greene, T., Croft, L.D., Neuhauser, M., Glassman, P., et al. (2017). Comparative effectiveness of vancomycin and metronidazole for the prevention of recurrence and death in patients with clostridium difficile infection. JAMA Intern. Med. *177*, 546–553.

Sundaram, K., Miller, D.P., Kumar, A., Teng, Y., Sayed, M., Mu, J., Lei, C., Sriwastva, M.K., Zhang, L., Jun, Y., et al. (2019). Plant-derived exosomal nanoparticles inhibit pathogenicity of porphyromonas gingivalis. iScience *21*, 308–327.

Teng, Y., Ren, Y., Sayed, M., Hu, X., Lei, C., Kumar, A., Hutchins, E., Mu, J., Deng, Z., Luo, C., et al. (2018). plant-derived exosomal microRNAs shape the gut microbiota. Cell Host Microbe *24*, 637–652.e8.

Valeri, M., and Raffatellu, M. (2016). Cytokines IL-17 and IL-22 in the host response to infection. Pathog. Dis. *74*, ftw111.

Vieco-Saiz, N., Belguesmia, Y., Raspoet, R., Auclair, E., Gancel, F., Kempf, I., and Drider, D. (2019). Benefits and inputs from lactic acid bacteria and their bacteriocins as alternatives to antibiotic growth promoters during food-animal production. Front. Microbiol. *10*, 57.

Wahlstrom, A., Sayin, S.I., Marschall, H.U., and Backhed, F. (2016). Intestinal crosstalk between bile acids and microbiota and its impact on host metabolism. Cell Metab. *24*, 41–50.

Wang, S., Xu, M., Wang, W., Cao, X., Piao, M., Khan, S., Yan, F., Cao, H., and Wang, B. (2016). Systematic review: adverse events of fecal microbiota transplantation. PLoS One *11*, e0161174.

Yang, C.H., Zhang, M.Z., and Merlin, D. (2018). Advances in plant-derived edible nanoparticle-based lipid nano-drug delivery systems as therapeutic nanomedicines. J. Mater. Chem. B *6*, 1312–1321.

Zelante, T., Iannitti, R.G., Cunha, C., De Luca, A., Giovannini, G., Pieraccini, G., Zecchi, R., D'angelo, C., Massi-Benedetti, C., Fallarino, F., et al. (2013). Tryptophan catabolites from microbiota engage aryl hydrocarbon receptor and balance mucosal reactivity via interleukin-22. Immunity *39*, 372–385.

iScience, Volume *23*

Supplemental Information

Lemon Exosome-like Nanoparticles-Manipulated Probiotics Protect Mice from *C. diff* Infection

Chao Lei, Jingyao Mu, Yun Teng, Liqing He, Fangyi Xu, Xiangcheng Zhang, Kumaran Sundaram, Anil Kumar, Mukesh K. Sriwastva, Matthew B. Lawrenz, Lifeng Zhang, Jun Yan, Wenke Feng, Craig J. McClain, Xiang Zhang, and Huang-Ge Zhang

Supplemental Information

Supporting figures

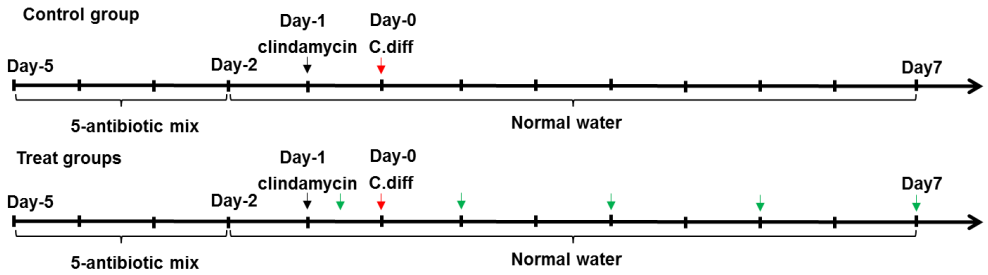

Fig. S1. Diagram of *C. diff* infection designs. Related to Fig.1, Fig.2 and Fig.3. Mice were treated with a mixture of 5 antibiotics (kanamycin 1 mg/ml, gentamicin 1 mg/ml, colistin 1 mg/ml, metronidazole 1 mg/ml, and vancomycin 0.5 mg/ml) for 3 days, followed with 1-day interval of normal water and then injected intraperitoneally with 0.2 mg clindamycin/mouse. Probiotics or LELN-probiotics were gavage-given to mice 12 h after the clindamycin injection and continued every two days (green arrows) for a total of 7 days. Mice were challenged with 100 *C. diff* spores at day-0 (red arrow).

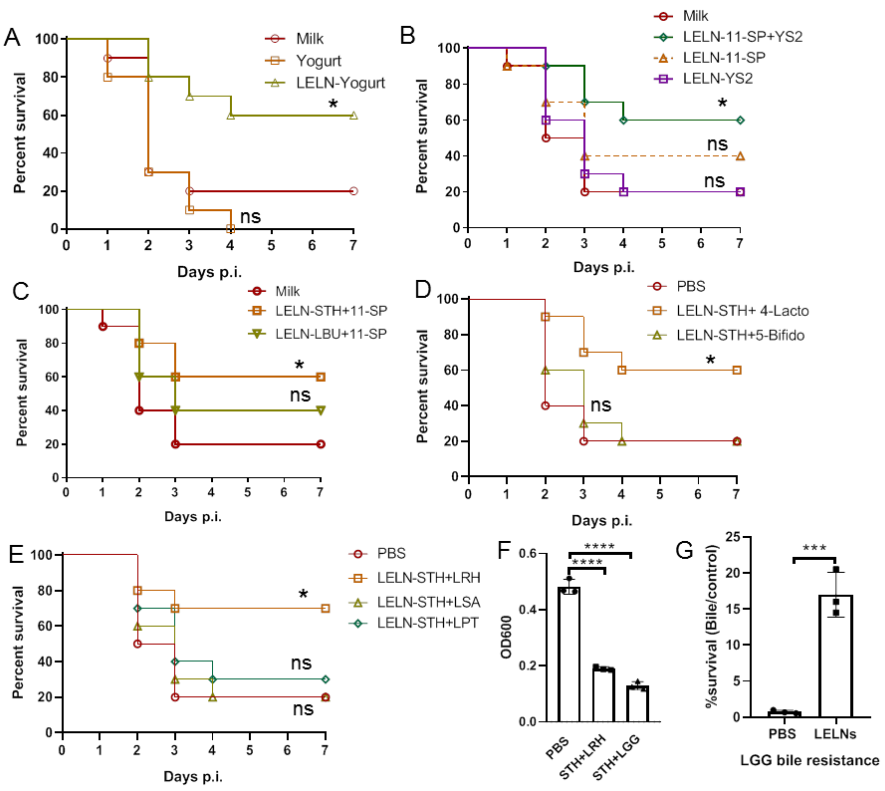

Fig. S2. Confirmation of the best probiotic combinations to protect mice against *C. diff* infection. Related to Fig.1. (A-E) Percent survival of *C. diff* infected mice under different treatments as indicated (n=10). (F) *in vitro* inhibition of *C. diff* growth by supernatant from co-cultures of STH and LRH, and co-culture of STH and LGG. (G) Bile resistance test of LGG with or without LELN pretreatment. The significance was analyzed using Log-rank (Mantel-Cox) tests for survival analyses, t-tests for two group analyses and ANOVA for multiple group analyses. The significance is shown as P≤0.05*, P≤0.01**, P≤0.001*** and P≤0.0001****. P>0.05 was considered to be not significant (ns). Data are representative of three independent experiments.

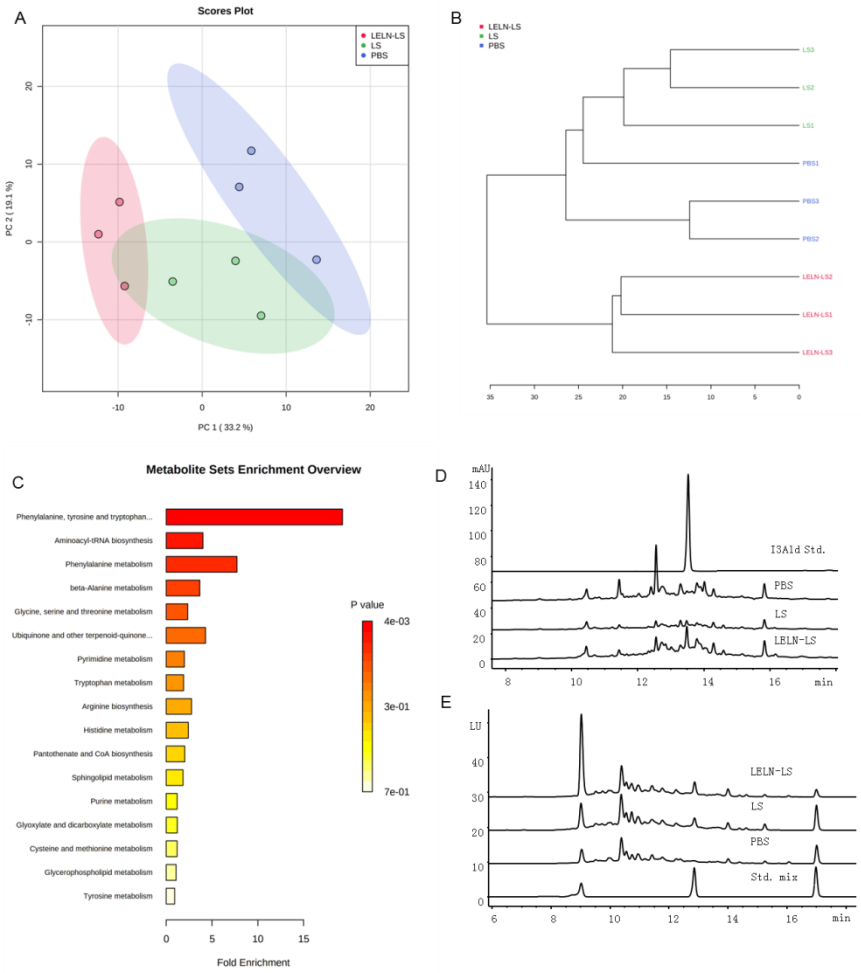

Fig. S3. Metabolomics analyses of colon content samples. Related to Fig.2. (A) PCA analysis (B) Dendrogram analysis and (C) Pathway enrichment analysis, all of these analyses were conducted using Metaboanalyst 4.0. (D-E) Determination by HPLC of tryptophan and tryptophan metabolites in the colon content samples. The standard mix (std. mix) contained tryptophan, I3LA and indole by the sequence of retention time.

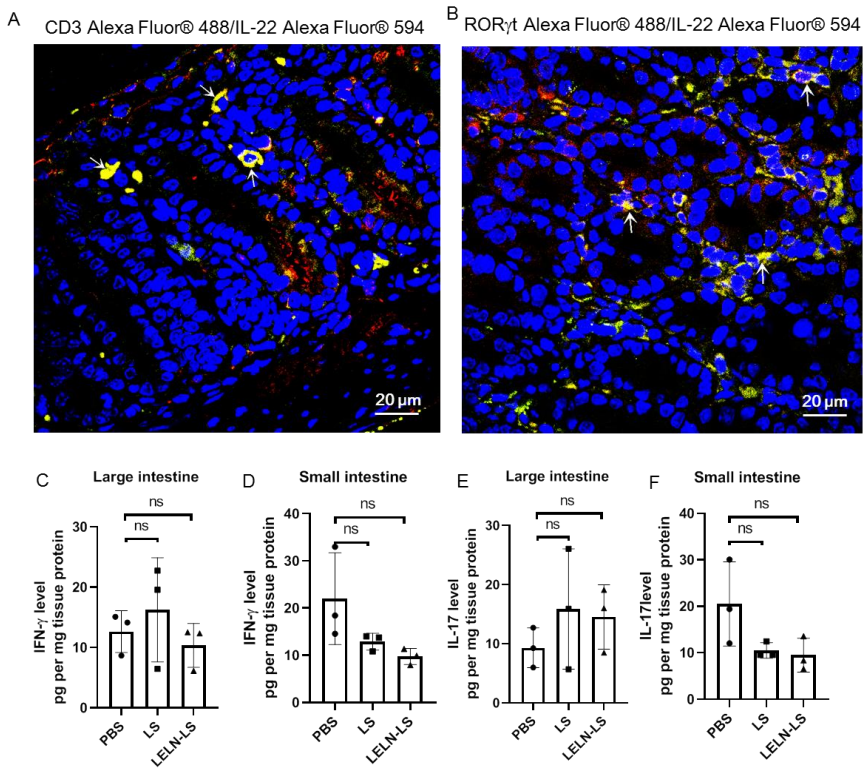

Fig.S4 LELN-LS effect on cytokine expression in the gut. Related to Fig.2. **(**A) Co-stain of CD3 and IL-22. (B) Co-stain of RORγt and IL-22. (C-F) ELISA analyses of IFN-γ and IL17 in the gut. The significance was analyzed using ANOVA for multiple group analyses. The significance is shown as P≤0.05*, P≤0.01**, P≤0.001*** and P≤0.0001****. P>0.05 was considered to be not significant (ns). Data are representative of three independent experiments.

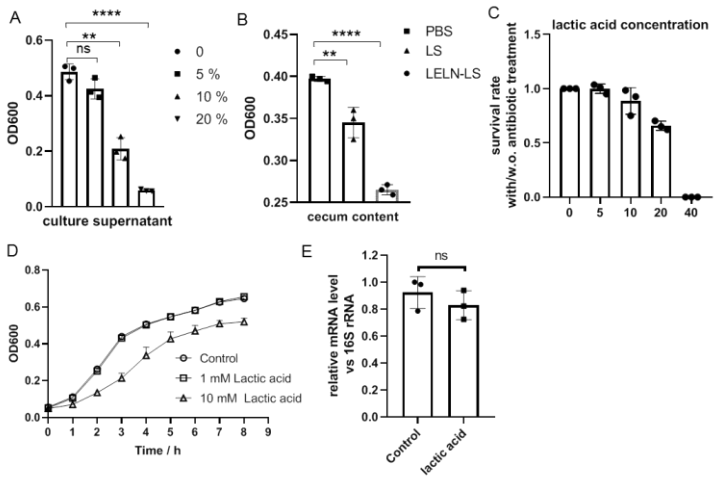

Fig. S5. Lactic acid produced by STH and LGG inhibit *C. diff* growth *in vitro*. Related to Fig.3. (A) Inhibition of *in vitro* of *C. diff* growth by supernatant of Co-LS, 3 different concentrations of supernatant were added as indicated. (B) Inhibition of *in vitro C. diff* growth by supernatant of cecum contents. (C) MIC test of lactic acid on *C. diff*. (D) Lactic acid effect on *E.coli* growth *in vitro*. (E) Lactic acid effect on *rpoD* gene expression. The significance was analyzed using ANOVA for multiple group analyses. The significance is shown as P≤0.05*, P≤0.01**, P≤0.001*** and P≤0.0001****. P>0.05 was considered to be not significant (ns). Data are representative of three independent experiments.

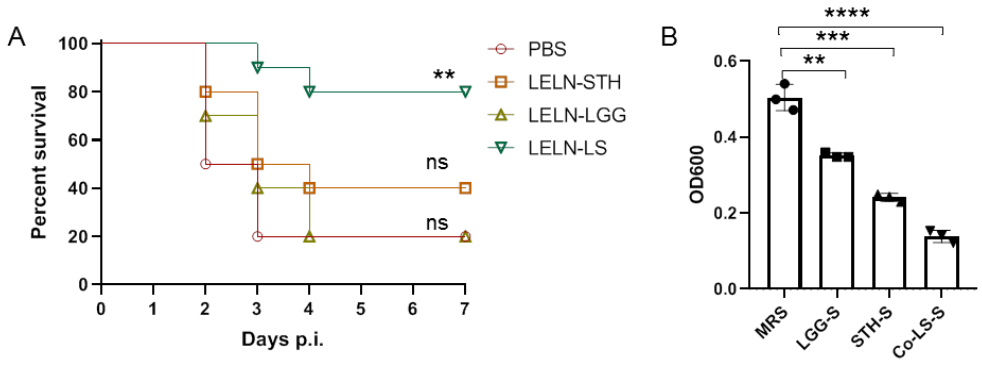

Fig.S6. Co-cultures of LGG and STH have the highest inhibition efficiency on the growth of *C. diff* and CDI. Related to Fig.4. (A) Percent survival of *C. diff* infected mice with different treatments as indicated. (B) Inhibition of *C. diff* growth by culture supernatant. Probiotic culture supernatants without LELNs pretreatment were added into *C. diff* inoculum up to 10% by volume. The significance was analyzed using Log-rank (Mantel-Cox) tests for survival analyses and ANOVA for multiple group analyses. The significance is shown as P≤0.01**, P≤0.001*** and P≤0.0001****. P>0.05 was considered to be not significant (ns). Data are represented as mean ± SD.

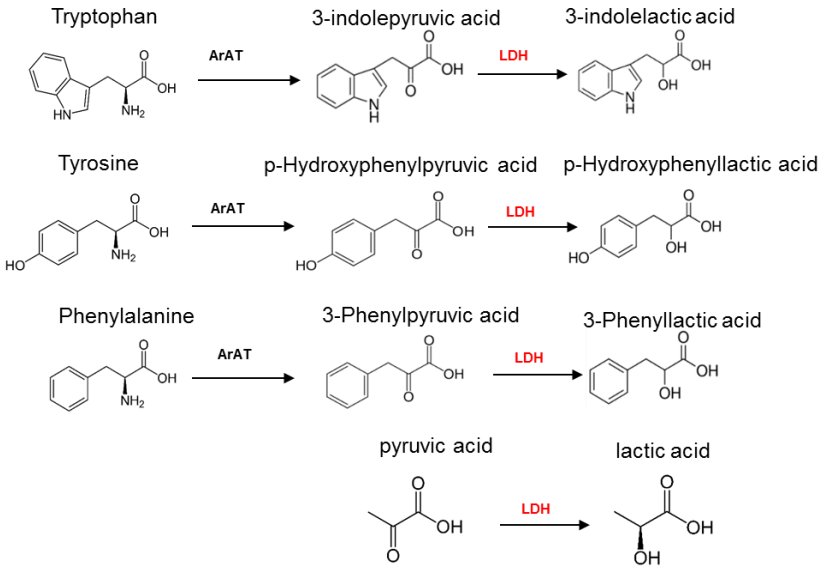

Fig.S7. Putative biosynthesis pathway of aryllactic acids from aromatic amino acids in lactobacilli. Related to Fig.4. ArAT, aromatic amino acid aminotransferase; LDH, lactate dehydrogenase.

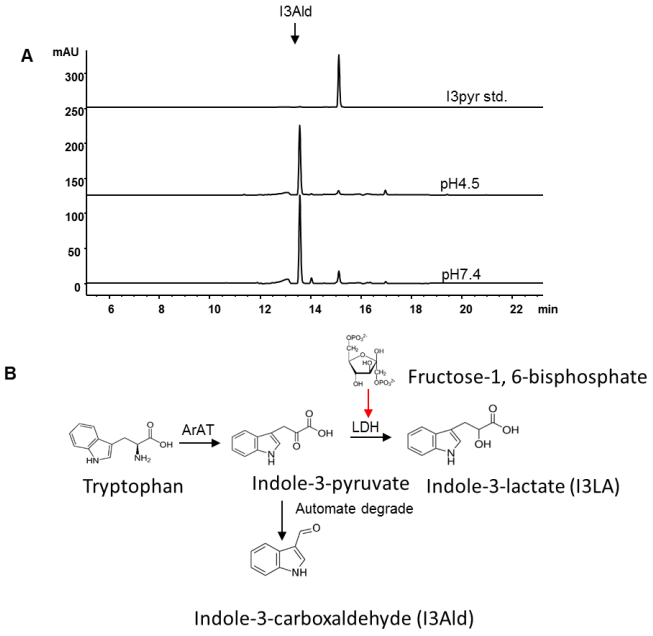

Fig. S8. Proposed biosynthesis pathway of I3LA and I3Ald in LGG. Related to Fig.4. (A) I3pyr auto-degradation test under two different pH, pH4.5 and pH7.4, for 2 h at 37 ℃. (B) proposed I3LA and I3Ald biosynthesis pathway. ArAT, aromatic

amino acid aminotransferase; LDH, lactate dehydrogenase; ID, indole-3-pyruvate decarboxylase.

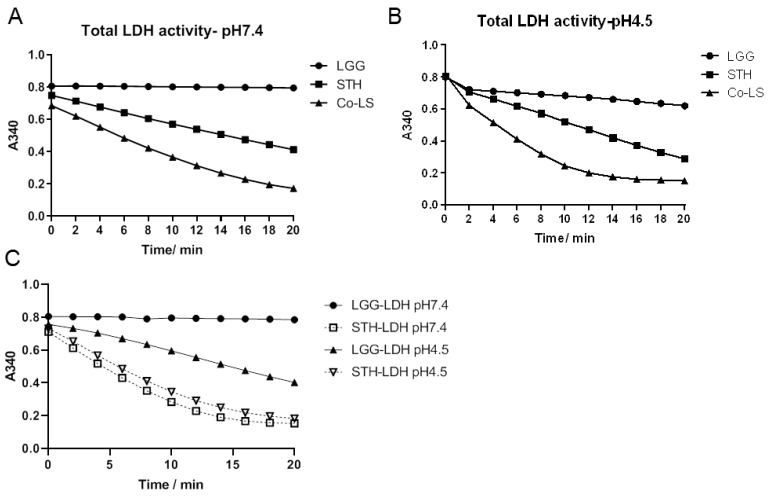

Fig.S9. Total LDH activities in the bacterial lysates. Related to Fig.4. (A-B) total LDH activities of different bacteria lysates at pH7.4 (A) and pH4.5 (B). (C) Comparison of total LGG-LDH and STH-LDH activities at two different pH as indicated. All the bacteria were collected after overnight culture at 37 ℃ and lysed by sonication.

Transparent Methods

Bacterial strains and culture conditions

E.coli and Top10 was purchased from Invitrogen; yogurt starter culture #2 (YS2), 11-strain probiotics (11-SP), 5-Bifidobacteria mix (5-bifido), 4-Lactobacillus mix (4-lacto), *Streptococcus thermophilus* ST-21 (STH), *Lactobacillus bulgaricus* LB-87 (LBU), and *Lactobacillus salivarius* LS-33 (LSA), *Lactobacillus plantarum* LP-115 (LPT) and *Lactobacillus rhamnosus* LR-32 (LRH) were purchased from Custom

Probiotics Inc.; *Lactobacillus rhamnosus* GG is stocked in our lab; and *C. diff* VPI 10463 was purchased from ATCC. *E. coli* was cultured in LB broth, *Lactobacilli* strains, *Bifidobacteria* strains and *Streptococcus thermophilus* were cultured in MRS without shaking, and *C. diff* was cultured in cooked meat broth under anaerobic conditions. All bacteria were cultured at 37 ℃.

LELNs extraction and purification from lemon fruit

Lemon fruit (*Citrus limon*) were purchased from a local Sam's Club market (#127308). LELNs were extracted and purified according to a previous report (Wang et al., 2014). LELN size distribution and quantity were determined using a Zetasizer Nano ZS (Malvern Instrument).

***C. diff* spore preparation**

C. diff spores were prepared according to a previous report (Perez et al., 2011). In briefly, *C. diff* was grown overnight in a 2 ml culture of Cooked Meat Broth (Sigma, cat: 60865-500G) at 37 ℃ anaerobically. The next day, the inoculum was added to 40 ml Clospore media and cultured anaerobically at 37 ℃ for 5-7 days to produce spores. Spores were then harvested by centrifugation and washed with cold water three times. The harvested spores were heat treated for 20 min at 65 ℃ to kill vegetative bacilli before being stored at -20 ℃. Viable spores were enumerated by plating on taurocholate, cefoxitin, cycloserine, fructose agar (TCCFA) to determine the infection dose.

Yogurt and probiotics culture preparation

Probiotic yogurts were prepared according to a previous report (Villarino et al., 2016). Briefly, 300 mg yogurt starter culture #2 (YS2) and 300 mg 11-strains probiotics (11-SP) were inoculated into 5 ml of 2% reduced fat milk and culture for 6-8 h at 37℃ until solidification. To prepare probiotic cultures, probiotic strains were inoculated into MRS broth and cultured for 24 h at 37℃ before being given to mice. For LELN pretreated yogurt or probiotic cultures, LELNs were added at a concentration of 1x 10^{10} /ml into the inoculum when starting the cultures. To determine effective probiotic strains in the yogurts, probiotics were grouped as YS2, 11-SP, 5-Bifido, 4-Lacto, LPT, LSA, LRH. LELN-Yogurt were made from grouped probiotics separately and combined to confirm protect effects on CDI.

Mice manipulation

8-week-old C57BL/6 female mice purchased from the Jackson Laboratory were used in our research except where otherwise stated. All mice experiments were conducted following the guidelines of the Institute for Laboratory Animal Research (ILAR). All protocols were approved by the University of Louisville Institutional Animal Care and Use Committee (Louisville, KY).

CDI mouse model

The CDI mouse model was conducted as previously reported (Chen et al., 2008). 8-week-old female B6 mice were treated with a mixture of five antibiotics (kanamycin (0.4 mg/mL), gentamicin (0.035 mg/mL), colistin (850 U/mL), metronidazole (0.215 mg/mL), and vancomycin (0.045 mg/mL)) for 3 days in their drinking water. Mice were then given 0.2 mg clindamycin one time by intraperitoneal

injection with 1-day interval of antibiotics stop. Mice were infected with 100 *C. diff* spores by gavage 24 h after the clindamycin injection.

Histological Analysis

Colon tissue were collected from *C. diff* infected mice and fixed at room temperature with 10% buffered formalin for 24 h. The colon tissue was dehydrated by sequential soaking in 70%, 80%, 95%, 100% ethanol for 45 min each time and then embedded in paraffin. The paraffin embedded colon tissue was then cut into ultrathin slices (5 mm) using a microtome. Hematoxylin and eosin (H&E) staining were conducted according to a previous report (Teng et al., 2018) and the slides were scanned with an Aperio ScanScope.

Gut permeability assay using FITC-Dextran

FITC dextran (mw. 4 KD) was purchased from Sigma (Cat: 46944). 8-week-old male C57BL/6J mice were used in the assay. 150 μl of 80 mg/ml FITC dextran was given to mice by gavage after a 4-6 h fast. Blood was collected 4 h after the FITC dextran gavage. 15% v/v acid-citrate-dextrose solution was used as an anticoagulant (38 mM citric acid, 107 mM sodium citrate, 136 mM dextrose). Plasma was prepared by centrifugation at 5,000 rpm for 10 min before being transferred to a new 1.5 mL microfuge tube. Fluorescence was determined at 530 nm with excitation at 485 nm using a spectrophotometer (BioTek-H1). Permeability was expressed as relative fluorescence units between the groups being compared.

Bile resistance assay

The bile resistance assay was performed as previously reported with minor modifications (Vinderola CG, 2003). In brief, STH was collected by centrifuge at 5,000x g for 5 min and washed twice with ice-cold 1x PBS to remove remaining broth. 1x 10^9 CFUs of STH were incubated with 0.2% porcine bile extract (Sigma, cat: B8631-100G) at 37 ℃ for 1 h and then washed twice to remove remaining bile before plating on MRS-Agar. To evaluate bile resistance, survival percentage of bacteria after bile treatment was determined using the Miles and Misra method (Miles et al., 1938).

Survivability of STH pass gastrointestinal tract

Mice were treated with an antibiotic mixture of vancomycin 0.5 mg/ml, ampicillin 1 mg/ml, streptomycin 1 mg/ml, neomycin 1 mg/ml, and metronidazole 1 mg/ml for 1 week to eliminate indigenous gut bacteria before STH gavage. 1 x 10^9 CFU STH or LELN-STH was given to mice by gavage 24 h after terminating the antibiotic treatment and fresh fecal samples were collected 24 h after gavaging the mice. STH CFUs were counted by serial dilutions and plated on MRS agar.

Metabolomics analysis

Colon content and culture broth samples were collected and prepared as described above. 300 µl of the samples were transferred to a fresh tube for lyophilization and the dried samples were reconstituted in 200 µl of 50% acetonitrile. The supernatant was used for 2DLC-MS/MS analysis after centrifuge at 13,000 rpm and passed through a 0.2 µm membrane filter. All samples were analyzed on a Thermo Q Extractive HF Hybrid Quadrupole-Orbitrap Mass Spectrometer coupled with a

Thermo DIONEX UltiMate 3000 HPLC system (Thermo Fisher Scientific). The metabolites were separated using the UltiMate 3000 HPLC system equipped with parallel dual columns as described previously (Klavins et al., 2014). Both positive mode (+) and negative mode (-) data were collected to obtain the full MS data of each metabolite. A pooled sample was prepared and analyzed by 2DLC-MS to acquire MS/MS spectra for metabolite identification. MetSign software was used for spectrum deconvolution, metabolite identification, and cross-sample peak list alignment. The threshold for the similarity of the MS/MS spectra between standards and pooled sample was set as ≥ 0.4, and the thresholds of retention time difference and m/z variation were set as ≤ 0.15 min and ≤ 4 ppm, respectively. The 2DLC-MS/MS data that failed to match our in-house database were then analyzed using Compound Discoverer software (Thermo Fisher Scientific), in which the threshold of MS/MS spectra similarity was set as ≥ 70 with a maximum score of 100. The metabolomics data normalization and statistical analyses were conducted using the Metaboanalyst 4.0 online tool (Chong et al., 2018).

Total RNA extraction and quantitative real time PCR

Total RNA was extracted using an RNeasy Mini Kit (Qiagen, cat: 74104) and following the manufacturer's instructions. For bacterial RNA, purified RNA was digested with 5 U RNase-free DNase I (NEB, cat: M0303S) for 30 min at 37℃ to remove remaining genomic DNA. DNase I was inactivated by incubating samples at 75℃ for 30 min. Reverse transcription was performed using SuperScript III First-Strand Synthesis System according to the manufacturer's instructions

(Invitrogen, cat: 18080051). Real time PCR was conducted using QuantiTect SYBR Green PCR Kits (Qiagen, cat: 204143) and run on a CFX96™ Real-Time PCR system (Bio-Rad).

ELISA assay for cytokines

Mucus was collected from small intestine and colon and homogenized in ice-cold 1x PBS by sonication. The supernatant was collected after centrifugation for 30 min at 13,000x g and protein concentration determined using a protein assay kit (Bio-Rad, cat: 500-0006). IL-22, IFN-γ, IL-17 levels were determined according to manufacturer's instructions (Invitrogen, cat: 88-7422-22; 88-7314-22; 88-7371-22) and normalized by total protein concentration in the samples.

Colon immune staining

Immune staining was conducted following the previous report (Teng et al., 2018). Briefly, colon tissues were collected and fixed with per-iodate-lysine-paraformaldehyde (PLP) for 2 h at room temperature. Fixed tissues were then embedded with O.C.T and make sections with 10 μm. Slides were incubated with 1% horse serum in PBS for 30 minutes at room temperature to block non-specific staining between the primary antibodies. Slides were then stained with primary antibodies overnight at 4℃(Rat anti-RORγt, Thermo Fisher Scientific, Cat:14-6988-80 1:500; Rabbit anti-IL22, Thermo Fisher Scientific, Cat:PA1-21357 1:500; Mouse anti-CD3 Thermo Fisher Scientific, Cat:14-0038-82, 1:500). Wash slides with PBS+0.1% Trition X-100 for 3 times and then stained with secondary antibodies (Anti-mouse Alexa Fluor® Plus 594, Thermo Fisher Scientific, Cat:A32744, 1:2000;

Anti-rabbit Alexa Fluor® Plus 488, Thermo Fisher Scientific, Cat:A32731, 1:2000; Anti-rat Alexa Fluor® Plus 594, Thermo Fisher Scientific, Cat:A-11007, 1:2000) for 2h at room temperature. Slides were mounted and scanned with Nikon Confocal Microscope.

Determination *C. diff* CFUs in the fecal samples

Fresh fecal samples were collected from *C. diff* infected mice and transferred into an anaerobic chamber immediately. Fecal samples were then homogenized in ice-cold and oxygen-depleted 1x PBS with concentration of 100 mg/ml. The suspension was held at room temperature for 5 min to remove large particles in the feces and 100 µl of the supernatant was plated on TCCFA plate by series dilution. The *C. diff* CFUs were determined after culturing for 24 h at 37 ℃.

Lactate concentration determination in culture broth and colon content samples

Lactate concentration in bacteria culture supernatant and gut contents was determined using a D-Lactate assay kit (Sigma, cat: MAK336) according to the manufacturer's instructions. For lactate detection in culture supernatant, the supernatant was collected from overnight broth cultures by centrifugation at 13,000x g for 30 min. For lactate detection in colon contents, fresh feces was collected from mice and homogenized in ice-cold 1x PBS and adjusted to a concentration of 100 mg/ml. Supernatants were collected after centrifugation at 13,000x g for 30 min. 20 µl of supernatant at an appropriate dilution were mixed with 80 µl reaction mixture and incubated 20 min at room temperature. The increase of absorbance at 565 nm was used to calculate lactate concentration in the samples.

Tryptophan and tryptophan-derived metabolite analysis by HPLC

Culture broth and colon content samples were collected and prepared as described above. Three volumes of ethanol were added to remove protein in samples. Tryptophan and tryptophan-derived metabolites were analyzed using reverse phase HPLC (RP-HPLC). RP-HPLC was performed on an Agilent 1260 system equipped with an Eclipse plus hexyl-phenyl column (4.6 mm x 150 mm, 5 μm). Deionized water with 0.1% formic acid and acetonitrile were used as the mobile phase. The gradients of the mobile phase were as follows: 0-5 min 5% acetonitrile, 5-15 min 5%-50% acetonitrile, 15-20 min 50% acetonitrile, 20-30 min 50%-95% acetonitrile, 30-35 min 95% acetonitrile, 35-38 min back to 5% acetonitrile, 38-40 min hold at 5% acetonitrile. Post-run was set to be 2 min. The flow rate and column temperature were set to be 1 ml/min and 30℃, respectively. Tryptophan and tryptophan-derived metabolites were detected using a fluorescence detector (Ex 280 nm, Em 350 nm) and DAD (UV=280 nm).

***In vitro* transformation of indole-3-pyruvic acid to indole-3-lactic acid by LDH**

Indole-3-pyruvic acid (cat: I7017-1G) and LDH derived from *Lactobacillus leichmannii* (cat: L3888-500UN) were purchased from Sigma. One mM indole-3-pyruvic acid, 11 μM NADH, 0.2 U LDH was mixed together in 100 mM acetate buffer (pH5.5). The reaction mix was held at 37℃ 30 min and the reaction stopped by adding 3 volumes of methanol. The transformation of indole-3-pyruvic acid to indole-3-lactic acid was detected by HPLC as described above.

C. diff* growth inhibition assay *In vitro

C. diff was inoculated into CM broth at a ratio of 1:100. Probiotic culture supernatant or chemicals were added into *C. diff* inoculum at the indicated concentration. To evaluate inhibition efficiency, the OD600 was determined after overnight culture at 37℃ under anaerobic conditions.

Minimal inhibitory concentration (MIC) of lactic acid

MIC of lactic acid was determined using the Agar Dilution Method as described previously with minor modifications (Andrews, 2001). Briefly, *C. diff* was inoculated on a CMB agar plate containing different concentrations of lactic acid and cultured at 37℃ in an anaerobic chamber. *C. diff* CFUs were counted after 24 h in culture to determine MIC. Lactic acid at concentrations of 0, 1, 10, 20, 40 mM were used in the assay.

Lactate dehydrogenase (LDH) activity assay *In vitro*

LDH activity was tested using an Enzymatic Assay of D-Lactic Dehydrogenase (Sigma, Cat: L-2011) following the manufacturer's instructions. Briefly, overnight cultured bacteria were collected by centrifugation and lysed by sonication. Supernatants of the lysates were collected after centrifugation at 13,000x g 30 min. Ten μg of total protein from lysate were mixed with 3.2 μM pyruvate, 0.8 μM NADH and incubated at 30℃. Absorbance at 340 nm was detected every 2 min for a total of 20 min. Two different buffer systems, 1x PBS (pH7.4) and 100 mM acetate buffer (pH4.5), were used in the test.

Intracellular FBP concentration determination by HPLC

Intracellular metabolites were extracted according to a previous report (Bennett et al., 2009). Briefly, bacteria were collected by centrifugation when the OD600=1.0. The bacteria were washed twice with ice-cold 1x PBS immediately. The intracellular metabolites were then extracted using a precooled acidic methanol/acetonitrile/water mixture solution (40:40:20 by volume in 0.1 M formic acid) and neutralized by ammonium hydroxide. FBP was determined by ion paired reverse phase HPLC (IP-RP HPLC) run over an Agilent 1260 system equipped with an Elipse plus C18 column (Agilent, 4.6 mm x 150 mm, 5 μm). Tributylamine was used as an ion pair reagent by adding it to the mobile phase. Mobile phase was A: 97 % water/3 % methanol containing 5 mM TBA and 5.5 mM acetic acid, and B: Methanol containing 5 mM TBA and 5.5 mM acetic acid. The gradients of the mobile phase were as follows: 3-3.5 min 0% B, 3.5-4 min increase to 30% B, 4-7.5 min hold 30% B, 7.5-8 min increase to 35% B, 8-15 min hold 35% B, 15-20 min increase to 99% B, 20-24 min hold 99% B, and post-run 5 min. FBP was detected using an Evaporative Light Scattering Detector (ELSD) with1.6 GSL nitrogen flow. Default parameters were used for ELSD.

Quantification and Statistics Analysis

All statistics analyses were performed using GraphPad Prism 8 software except where otherwise stated. The data are presented as values with standard deviation (mean ± SD). The significance was analyzed using Log-rank (Mantel-Cox) tests for survival analyses, t-tests for two group analyses and ANOVA for multiple group analyses. The significance is shown as $P \leq 0.05$*, $P \leq 0.01$**, $P \leq 0.001$*** and $P \leq 0.0001$****. $P > 0.05$

was considered to be not significant (ns). Data are representative of three independent experiments.

Supplemental references

ANDREWS, J. M. 2001. Determination of minimum inhibitory concentrations. *J Antimicrob Chemother,* 48 Suppl 1**,** 5-16.

BENNETT, B. D., KIMBALL, E. H., GAO, M., OSTERHOUT, R., VAN DIEN, S. J. & RABINOWITZ, J. D. 2009. Absolute metabolite concentrations and implied enzyme active site occupancy in Escherichia coli. *Nat Chem Biol,* 5**,** 593-9.

CHEN, X., KATCHAR, K., GOLDSMITH, J. D., NANTHAKUMAR, N., CHEKNIS, A., GERDING, D. N. & KELLY, C. P. 2008. A mouse model of Clostridium difficile-associated disease. *Gastroenterology,* 135**,** 1984-92.

CHONG, J., SOUFAN, O., LI, C., CARAUS, I., LI, S., BOURQUE, G., WISHART, D. S. & XIA, J. 2018. MetaboAnalyst 4.0: towards more transparent and integrative metabolomics analysis. *Nucleic Acids Res,* 46**,** W486-W494.

KLAVINS, K., DREXLER, H., HANN, S. & KOELLENSPERGER, G. 2014. Quantitative metabolite profiling utilizing parallel column analysis for simultaneous reversed-phase and hydrophilic interaction liquid chromatography separations combined with tandem mass spectrometry. *Anal Chem,* 86**,** 4145-50.

MILES, A. A., MISRA, S. S. & IRWIN, J. O. 1938. The estimation of the bactericidal power of the blood. *J Hyg (Lond),* 38**,** 732-49.

PEREZ, J., SPRINGTHORPE, V. S. & SATTAR, S. A. 2011. Clospore: a liquid medium for producing high titers of semi-purified spores of Clostridium difficile. *J AOAC Int*, 94**,** 618-26.

TENG, Y., REN, Y., SAYED, M., HU, X., LEI, C., KUMAR, A., HUTCHINS, E., MU, J., DENG, Z., LUO, C., SUNDARAM, K., SRIWASTVA, M. K., ZHANG, L., HSIEH, M., REIMAN, R., HARIBABU, B., YAN, J., JALA, V. R., MILLER, D. M., VAN KEUREN-JENSEN, K., MERCHANT, M. L., MCCLAIN, C. J., PARK, J. W., EGILMEZ, N. K. & ZHANG, H. G. 2018. Plant-Derived Exosomal MicroRNAs Shape the Gut Microbiota. *Cell Host Microbe*, 24**,** 637-652 e8.

VILLARINO, N. F., LECLEIR, G. R., DENNY, J. E., DEARTH, S. P., HARDING, C. L., SLOAN, S. S., GRIBBLE, J. L., CAMPAGNA, S. R., WILHELM, S. W. & SCHMIDT, N. W. 2016. Composition of the gut microbiota modulates the severity of malaria. *Proc Natl Acad Sci U S A*, 113**,** 2235-40.

VINDEROLA CG, R. J. 2003. Lactic acid starter and probiotic bacteria: a comparative "in vitro" study of probiotic characteristics and biological barrier resistance. *Food Research International* 36**,** 895-904.

WANG, B., ZHUANG, X., DENG, Z. B., JIANG, H., MU, J., WANG, Q., XIANG, X., GUO, H., ZHANG, L., DRYDEN, G., YAN, J., MILLER, D. & ZHANG, H. G. 2014. Targeted drug delivery to intestinal macrophages by bioactive nanovesicles released from grapefruit. *Mol Ther*, 22**,** 522-534.